International Journal of Chemical and Biochemical Sciences
(ISSN 2226-9614)

Journal Home page: www.iscientific.org/Journal.html

The Impact of Atorvastatin and Cinnamon on the Hypercholesterolemic Albino Rats' Submandibular Salivary Gland

Asmaa Ahmed Foad[1], Elham Fathy Mahmoud[2], Mervet Mohammed Hawwas[3], Abdel Nasser Mohammed Hashem El-Refai[4], Enas Hegazy[5]*

[1]*PHD Faculty of Dentistry, Beni Suef University.*

[2]*Professor of Oral Biology, Faculty of Dentistry, Suez Canal University.*

[3]*Professor of Oral Biology, Faculty of Dentistry, Suez Canal University.*

[4]*Professor of Oral Medicine, Faculty of Dentistry, Suez Canal University.*

[5]*Assoc. Professor of Oral Biology, Faculty of Dentistry, Suez Canal University.*

Abstract

This study examines the effects of atorvastatin and cinnamon on the submandibular salivary gland in albino rats with high cholesterol, highlighting the potential of plant extracts in managing hypercholesterolemia. Blood cholesterol levels and submandibular gland tissue were both positively impacted by the synthetic treatment of Atorvastatin for hypercholesterolemia. In hypercholesteraemic rats, cinnamon improved blood cholesterol levels, the histological and ultrastructure picture of the submandibular gland, and the amount of caspase III when used as a natural herbal remedy.

Keywords: Atorvastatin, Cinnamon, Caspase III, Submandibular Salivary Gland, Hypercholesterolemia.

Full length article **Corresponding Author*, e-mail: asmaahmedfoad14@gmail.com

1. Introduction

Cholesterol, a lipid, preserves cellular membrane fluidity, aids embryo and fetus development, and contains bioactive compounds like bile acids, vitamin D, and steroid hormones [1]. Herbal therapies and synthetic pharmaceuticals are both effective in treating hypercholesterolemia. Among the synthetic medications used worldwide to treat dyslipidemia are statins, which inhibit the action of HMG CoA reductase [2]. As per Qiu et al., (2017), atorvastatin is a statin that is suggested for managing different types of dyslipidemias such as adult mixed dyslipidemia, hypertriglyceridemia, primary lipoproteinemia, homozygous familial hypercholesterolemia, and heterozygous familial hypercholesterolemia in adolescents [3]. Traditional plant-based medicine in Asian nations, like Cinnamomum burmannii, may have anti-diabetic effects and lower blood sugar levels due to its potent lipolytic action, which influences lipid metabolism and potentially lowers cholesterol levels [4].

2. Materials and Methods

2.1 Materials preparation

2.1.1. Preparation of Cholesterol Rich Diet

The recipe for a cholesterol-rich meal included the following ingredients: 10 grams of cholesterol, 120 grams of casein, 50 grams of salt mixture, 10 grams of vitamin mixture, 250 grams of soybean oil, 0.4 grams of choline, 130 grams of cellulose, and 429.6 grams of corn starch. Bile salt mixture, which is required for the intestinal absorption of cholesterol, was also added [5].

2.1.2. Preparation of Atorvastatin

Atorvastatin tablets were crushed by mortar and pistol and dissolved in a distilled water in a concentration of 10% and were administrated by oropharyngeal tube [6].

2.1.3 Preparation of Cinnamon

The powder was dried, diluted in 10% distilled water, and delivered via oropharyngeal tube. It was purchased from the Harraz local market in Cairo [7].

2.2. Methods

2.2.1. Sample Size Calculation

The G* Power version 3.19.2, Franze Faul, University Kiel, Germany, will be used to calculate the sample size. © 1992-2014 Copyright. With a power of 95% and an effect size of 0.8 utilizing both the beta (β) and α levels of 0.05, the estimated sample size (n) should consist of at least 60 rats divided into 6 groups, with 7 rats in each group.

2.2.2. Study Design

There were twenty-one mature male albino rats at the start of the trial, weighing between 160 and 180 grams each. Prior to the trial, the rats were given a week of acclimation. Each of the five rats was kept in a separate cage with adequate ventilation. Throughout the trial period, a sufficient diet consisting of fresh vegetables, dried bread, and tap water was freely available. From the time of their lodging until their termination, which was handled by the incinerator, this was carried out under the observation of a trained animal caregiver.

2.3. Animal Grouping and Handling Procedure

Rats were split evenly into the following two major groups:

2.3.1. Control group

Seven rats in this group received distilled water through an orophayngeal tube and a regular meal for four months.

2.3.2. Experimental groups

2.3.2.1. 2-A Cholesterol-rich diet group

1% powdered cholesterol was included in the high-cholesterol diet that the seven rats in this group were fed for four months [8].

2.3.2.2. 2-b Cholesterol-rich diet + Atorvastatin group

The atorvastatin tablets were administered by oropharyngeal tube after being crushed with a mortar and pestle and diluted in 10% distilled water [6].

2.3.2.3. 2-C Cholesterol-rich diet + Cinnamon group

A 10% concentration of dried powder was dissolved in distilled water and administered via an oropharyngeal tube (Figure 4) after being purchased from the Harraz local market in Cairo [7].

3. Results

3.1 Biochemical Analysis

After the third and fourth months, the mean plasma cholesterol level for all groups revealed the following before hypercholesterolemia was induced: Prior to the production of hypercholesterolemia, plasma cholesterol levels were the same in all groups, and the t-test revealed a negligible statistical difference between the groups. The control group's mean plasma cholesterol level was lower than that of the other groups following the induction of hypercholesterolemia. At the conclusion of the fourth month, the average plasma cholesterol level in the cholesterol group was considerably higher than in the other groups. The cholesterol+Atorvastatin group showed a significant decrease in comparison to the cholesterol group; however, there was no difference between the cholesterol. At the conclusion of the study period, lipid profiles were assessed both prior to and following the development of (Table 1 & Figure 1).

3.2. Histological Results

3.2.1. Control group

The parenchyma of the submandibular gland is made up of secretory end pieces and collecting ducts, with intercalated ducts having narrow lumens and cuboidal cells with basally located nuclei and striated ducts made up of columnar cells with centrally located open-faced nuclei, according to an examination of H & E-stained sections (Figure 2A).

3.2.2. Cholesterol-rich diet group

A set of cells underwent microscopic inspection, which showed aberrant mitosis, broken borders, vacuolar degeneration, conspicuous chromatin, and lack of typical acinar cell layout. Whereas striated duct cells had no basal striations and an aberrant architecture with ill-defined borders, intercalated duct cells had both of these characteristics. The cytoplasm was deteriorated and majority of the nuclei had necrotic areas with vacuolated cytoplasm. Necrotic cells, indistinct borders, and a loss of normal architecture were also observed in granular convoluted tubules (Figure 2B).

3.2.3. Cholesterol-rich diet+ Atorvastatin

Histological analysis performed on the group showed a restoration to normal secretory cell arrangement into spherical-shaped acini, as well as typical acinar appearance. Acinar cells lost their cellular borders and pyramidal structure, and some serous acini had burst cells. The intercalated duct displayed a narrow lumen and typical cell borders (Figure 2C). The investigation revealed basal striations, striated ducts with returning normal cell borders, and granular convoluted tubules with normal histological structure (Figure 2C).

3.2.4. Cholesterol-rich diet + Cinnamon

Sections stained with hematoxylin and eosin revealed the gland's usual structural characteristics, including a regular arrangement of secretory acini and ducts. The striated duct cells possessed distinct borders and basal striations, but the intercalated duct had typical histological characteristics. A few ducts continued to secrete. The granular convoluted tubule featured towering columnar cells, a large lumen, and regular borders (Figure 2D).

3.3. Immunohistochemical Results

A negative to weak immune response was observed in rats given a regular diet for four months, according to the qualitative analysis of color intensity immunoreaction to caspase III. The group that consumed a diet high in cholesterol exhibited strong to moderate positive immune responses, and at the conclusion of the fourth month, the mean anti-caspase immune response in the submandibular salivary gland demonstrated a significant rise when compared to the other groups.

After receiving atorvastatin tablets for a month, hypercholesterolemic rats demonstrated strong to moderate immunoreactivity; the difference between this group and the cholesterol group was not statistically significant. Cinnamon-treated hypercholesterolemic rats had a weakened immunological response to the caspase III antibody. There is a significant distinction between cinnamon treated group and the cholesterol group (Table 2).

3.4. Transmission Electron Microscope Results

3.4.1. Control Group

A rat's submandibular salivary gland displayed normal ultrastructural features, including pyramidal cells and spherical acini with a central constricted lumen. Both basally and laterally located golgi bodies were seen, and the electron concentrations of free ribosomes and lysosomes varied. Round euchromatic nuclei surrounded by many mitochondria were found in the basal portion of the cells (Figure 4A). Tall columnar cells with big, spherical nuclei lined the granular convoluted tubules. Numerous tightly packed membrane-bound granules were seen (Figure 4B).

3.4.2. Cholesterol-rich diet group

When the submandibular salivary glands of a diet heavy in cholesterol were studied, atrophic alterations were observed in the serous secretory cells. Cytoplasmic vacuolations and uneven pyramidal morphology characterized the acinar cells. Widening intercellular connections, loss of mitochondria, and organelle degeneration were seen in some acini. An absence of interdigitation was also found in the study (Figure 4B). According to the study, granular convoluted tubules had suffered significant damage. Damage to the rough endoplasmic reticulum, mitochondria, and other organelles was shown by numerous cell vacuolization.

3.4.3. Cholesterol-Rich Diet + Atorvastatin Group

When the cholesterol-rich diet group taking atorvastatin had their submandibular salivary gland examined under an electron microscope, the ultrastructural elements were comparatively restored to normal. In this group of rats, the submandibular salivary gland's serous acini displayed enormous pyramidal cells with nuclei that were nearly spherical at the base. Relative intercellular connections were visible in the cell membranes of the nearby cells, as seen by a large number of integrations and desmosomes (Figure 4 C). Numerous cytoplasmic granules were visible, and columnar cells with a basally positioned nucleus lined the granular convoluted tubules.

3.4.4. Cholesterol Rich Diet + Cinnamon

The serous acini of the rat's submandibular salivary gland in the cholesterol-rich diet group that received cinnamon treatment were observed under an electron microscope to have big pyramidal cells with an almost rounded basally situated nucleus (Figure 4D). Columnar cells with a basally positioned nucleus lined the granular convoluted tubules. Liquid stagnation is present in the lumen, which is surrounded by cells. There were numerous large-sized and freshly produced cytoplasmic granules visible. While some of the freshly produced mitochondria were visible, others were scattered.

4. Discussion

According to prior study findings published by Khosla and Sundram (1996), who employed albino rats fed on various amounts and kinds of fats, feeding albino rats a high-fat meal including cholesterol crystals, they produced hypercholesterolemia in the diet group high in cholesterol [9]. The current investigation found that adding supplements to a diet rich in cholesterol was sufficient to result in hyperlipidemia. Iqbal and Mudassar (2015) published similar findings demonstrating increased blood lipid profile values in rats and rabbits on a high-cholesterol diet [10]. The submandibular salivary gland of albino rats given a high-fat diet for four months was examined histologically and ultrastructural to determine how the high-fat diet affected the gland's histological structure and led to the loss of the typical morphology of acinar cells. It was discovered that a high-fat diet causes significant changes in the parotid salivary gland, leading to lipid buildup and inflammatory responses, potentially limiting oxygen and food molecules, and negatively impacting cell function and survival [11]. The study suggests that intracellular lipids cause vacuoles, which may be due to degenerative changes in secretory cells. This aligns with previous research suggesting that high-fat diets cause lipid accumulation in secretory cells. Salivary glands accumulate lipid droplets, causing pressure on acini boundaries and resulting in eroded and deformed structures [12]. On the ultrastructural evaluation scale, it was proposed that cytoplasmic vacuolization is a physiological adaptation to limit harm, starting with tiny vesicles fused into larger vacuoles. Following hypotonic shock, cells' distended mitochondria give them a vacuolated appearance, impacting the endoplasmic reticulum and Golgi apparatus [13]. Rats fed a high-fat diet show significant changes in their submandibular salivary gland, resulting from lipid droplet pressure and increased salivary secretion. This is linked to glandular dysfunction and abnormal secretory duct degeneration [14]. It was explained that dilated striated ducts and stagnate excretion may be due to mitochondrial injury, ATP depletion, membrane pump failure, and biosynthesis failure. This lack of energy leads to ductal dilatation and obstruction, resulting in the transfer of secretions by cells [15]. Red blood cells were found in dilated blood arteries in a group with hypercholesterolemia, consistent with previous studies showing cellular infiltration and dilated blood channels congested with red blood cells in hypercholesterolemic rats, possibly due to an inflammatory response to improve blood supply to degeneration areas [11]. Ultrastructural analysis revealed dilated rough endoplasmic reticulum (RER) in some acini, with severe organelle degeneration and weak intercellular connections. This aligns with previous studies showing that a lipid-rich diet in rats leads to recessed, compressed nuclei with little or no euchromatin, indicating a potential link between lipid-rich diets and acinar cell dysfunction [16]. The marked dilatation of the rough endoplasmic reticulum (RER) was also explained by Selim, who confirmed that the RER's enlargement is related to the cellular condition that occurs before apoptotic manifestations [17]. Electron microscopy research indicates that the packing of mitochondria between plasma membrane basal infoldings causes striated duct cell basal striations, which could be lost due to mitochondrial damage caused by oxidative stress [18].

The study's immunohistochemical results confirmed the findings in the hypercholesterolemic group, with caspase III antibodies showing strong to moderate positive reactions to activated caspase III in acinar and ductal cells, connective tissue cells, and endothelial cells. Research suggests that strong to moderate immune reactivity in this population may be due to the activation of "death domain" receptors, such as TNFR-1 or FAS, by cytokines, possibly due to hypercholesterolemia [19]. The study suggests that hypercholesterolemia can lead to increased oxidative stress, causing excessive reactive oxygen species (ROS) development and severe oxidation of cell lipids, proteins, and DNA. This, through caspase III activation, results in apoptosis, a common pathogenic outcome in hypercholesterolemia [20]. On the other hand, Jang et al., (2002) added that caspase III has several cellular targets, and upon activation, caspase III results in morphologic characteristics of apoptosis [21]. The study involved albino rats fed a high-fat diet for three months, who were given a month of treatment with 10 mg/kg BW Atorvastatin tablets, a favored clinical lipid-regulating medication. AL-Rawi (2007) reported that in patients with hyperlipidemia, atorvastatin effectively reduces abnormal blood cholesterol levels, inhibits the development of atherosclerosis, and reduces clinical cardiovascular events [22]. In comparison to the cholesterol group, this group's biochemical data indicated a substantial drop in total cholesterol, LDL, and HDL levels. Studies have shown that statins inhibit HMG-CoA reductase, lowering cholesterol levels and increasing protease activity. This leads to increased sterol regulatory element binding protein (SREBP) entry into the endoplasmic reticulum, regulating the amount of circulating LDL [23]. Researchers have also shown that statins reduce LDL by blocking the liver from generating the LDL receptors known as apolipoprotein B-100. When LDL receptors are not working in persons with hypercholesterolemia, atorvastatin can reduce LDL [24-27]. In the present experiment, histological and ultrastructural examination of hypercholesterolemic r34.s treated with Atorvastatin showed that the normal structural features of the gland were almost treated to their normal features. The return of typical acinar appearance with its histological features in this group was explained by Laufs et al., (1998), Who claimed that endothelial dysfunction is a precursor to atherosclerotic lesions, which are brought on by high cholesterol. The ability of endothelial cells to generate nitrous oxide (NO), which controls the endothelium's anti-atherosclerotic activity, is decreased by hypercholesterolemia [28]. Previous findings were reported by Wagner et al., (2000), who proposed that statins change the NO-/ O2- balance by stopping endothelial cells from producing O2, which then allows endothelial cells to function again [27]. Histological and ultrastructural examination of this group showed the return of the Intercalated, striated, and excretory ducts to their normal histological features. The study supports previous research indicating statins improve blood flow control and lipid profile modification, leading to increased endothelium-dependent vasodilation, tissue repair, and the development of new blood vessels [29-30]. Histological analysis revealed dilated granular convoluted tubules in the same group, with cytoplasmic vacuolar degeneration in some. However, cell borders and nuclei were only slightly normal in other granular tubules, attributed to studies showing that statins reduce cholesterol and coenzyme Q10 production in hypercholesterolemia patients [31-34]. Vascular degenerative signs of the granular convoluted tubule and some acinar cells may be because of what Kumar (2007) showed that treatment with atorvastatin caused pancreatic acinar degeneration in hyperlipidemic rats in various degrees, resulting in the loss of their normal architecture and empty spaces between the pancreatic acini. Acinar cells might have unclear cell borders. It clarifies the implications of the poor histology data [35]. The study found that high-fat diet rats treated with Atorvastatin showed strong to moderate immunoreaction against caspase III, consistent with Chen et al. (2014). who found that atorvastatin improved left ventricular function, reduced infarct size, and decreased cell apoptosis in rats with experimental acute myocardial infarction [36]. The Bcl-2 family in the endoplasmic reticulum regulates various signaling pathways and cell viability. Anti-apoptotic proteins like Bcl-2 may explain their moderate to poor response to various apoptosis inducers [37]. It is now regular practice to employ plant extracts to treat various illnesses. Additionally, many plant materials are used as supplements. In this research, albino rats fed a high-fat diet for 4 months were treated with 6 mg/kg. BW cinnamon powder. Using 6 mg cinnamon powder in agreement with Khan et al., (2003) findings, they discovered that cinnamon bark's potent lipolytic action helped type 2 diabetic individuals lower their free fatty acid levels and manage their total cholesterol and triglyceride levels at varied dosages. This proves that cinnamon powder effectively avoids hyperlipidemia's elevated lipid profile levels [38]· The study found that when cinnamon powder was administered to hypercholesterolemic rats, plasma cholesterol and LDL levels decreased by 54%, LDL decreased by 211 mg/dl to 61 mg/dl, and HDL increased dramatically from 36 mg/dl to 63 mg/dl [39]. In addition, Khan et al., (2003) revealed that cinnamon medication directly impacts how lipids are metabolized. Thanks to its potent lipolytic action, cinnamon protects against hypercholesterolemia and hypertriglyceridemia and decreases levels of free fatty acids and TG [38]. The ultrastructural analysis reveals columnar cells bordering striated channels, with radially distributed mitochondria and complex infoldings. Cinnamon's active ingredient controlling mitochondrial permeability may contribute to the observed advancement in mitochondrial structure [40].

Table 1: Showing mean plasma cholesterol level before induction of hypercholesterolemia, at the end of third month, at the end of the fourth month.

	Before induction of hypercholesterolemia	At the end of the third month	At the end of the fourth month
Control	97.432	98.857	99.125
Cholesterol rich diet	97.28	165.542	233.525
Cholesterol + Atorvastatin	95.142	166.828	115.202
Cholesterol + Cinnamon	96.000	165.943	113.584

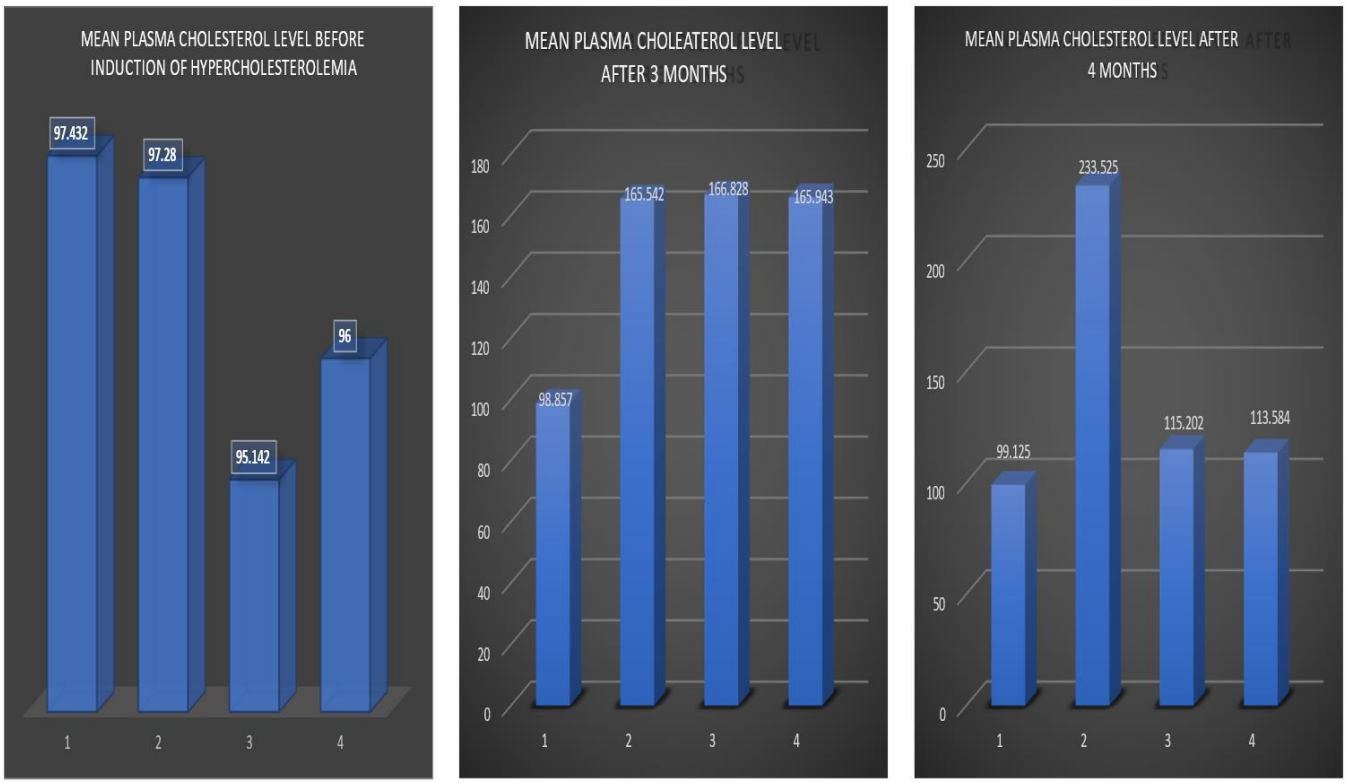

Figure 1: Before hypercholesterolemia induction, at the end of the third month, and at the end of the fourth month, for each group, the mean plasma cholesterol levels are displayed.

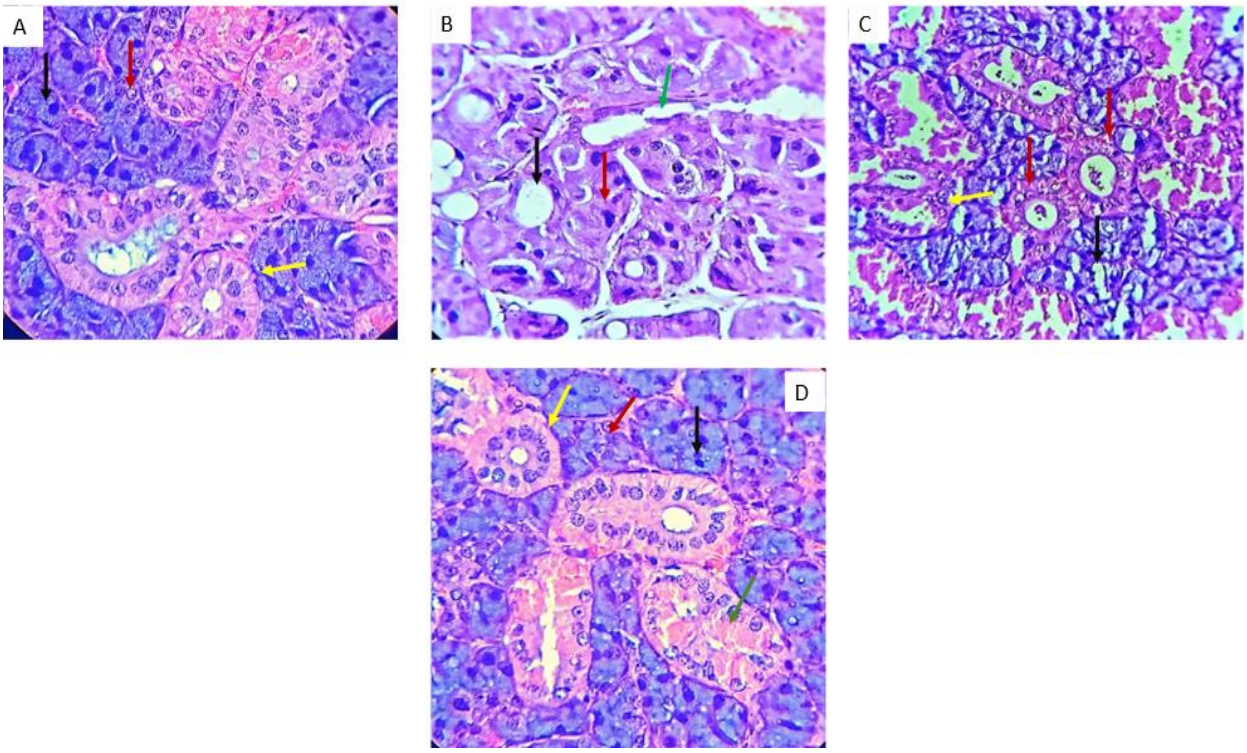

Figure 2 (A): A photomicrograph displaying serous acini (black arrow) in the control group, (B): A photomicrograph of the cholesterol group displaying degenerated acini (black arrow), striated duct with loss of basal striations (red arrows), degenerated convoluted tubule (yellow arrow), (C): A photomicrograph of the atorvastatin-treated group demonstrating serous acini with cytoplasmic vacuoles (black arrows), an intercalated duct (yellow arrow), and striated ducts with basal striations (red arrows), as well as isolated striated ducts with loss of basal striation (black arrows), dilated blood vessel congested with RBCs (green arrow), (D): A photomicrograph of the cinnamon-treated group demonstrating spherical acini (black arrows), conventional intercalated duct (red arrow) (H & E, x 400).

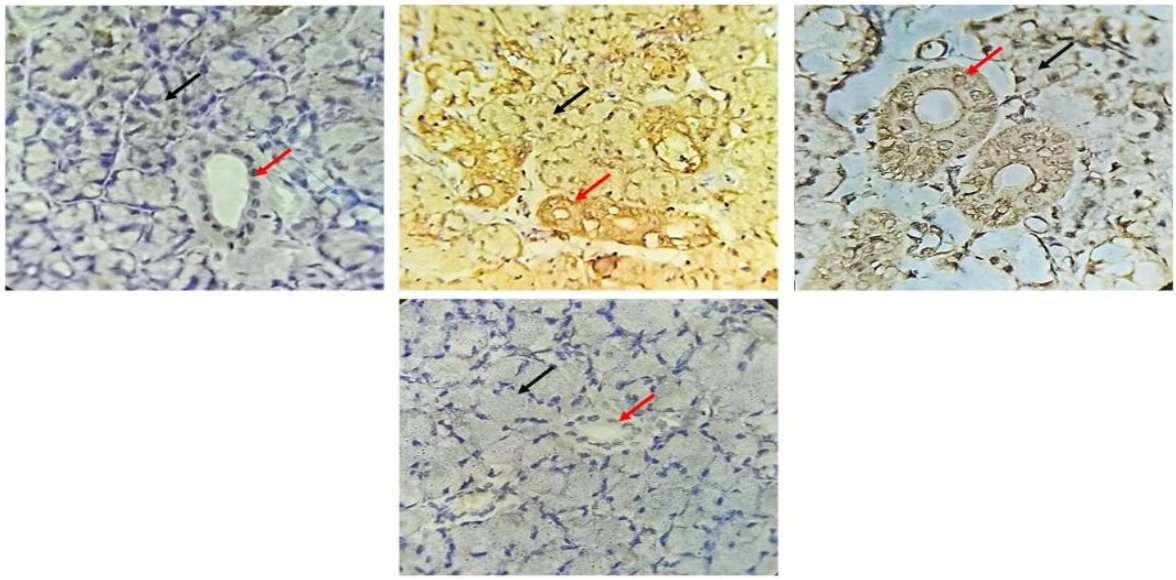

Figure 3 (A): A photomicrograph of the control group demonstrating a mild to negative immune response within the acinar cells' cytoplasm (black arrow) and striated duct (red arrow) examples of duct cells, (B): A photomicrograph of the cholesterol group demonstrating cytoplasm of striated (red arrow) and acinar cytoplasm (black arrow), as well as a strong to moderate immunological response at the basement membrane, (C): Photomicrograph of the atorvastatin-treated group demonstrating a moderate to weak immune response at the cytoplasm of acinar cells (black arrow) and striated duct (red arrow) (caspase III org. mag. 640).

Table 2: Average of the various experiment groups' submandibular salivary gland Caspase III immune response.

	Mean	Std. Deviation	Std. Error	95% Confidence Interval Lower Bound	Upper Bound	Color Intensity Percentage
Control group	32.4324	8.757215	0.380829579	-1.369438919	0.745265922	5.07%
Cholesterol	129.5476	24.20065	0.492517234	-1.41101364	1.323880489	45.55%
Cholesterol + Atorvastatin	43.1716	7.398703	0.746366778	-2.515255232	1.629237545	15.18%
Cholesterol + Cinnamon	28.144	15.83386	0.661310698	-1.273396119	2.39878958	13.75%

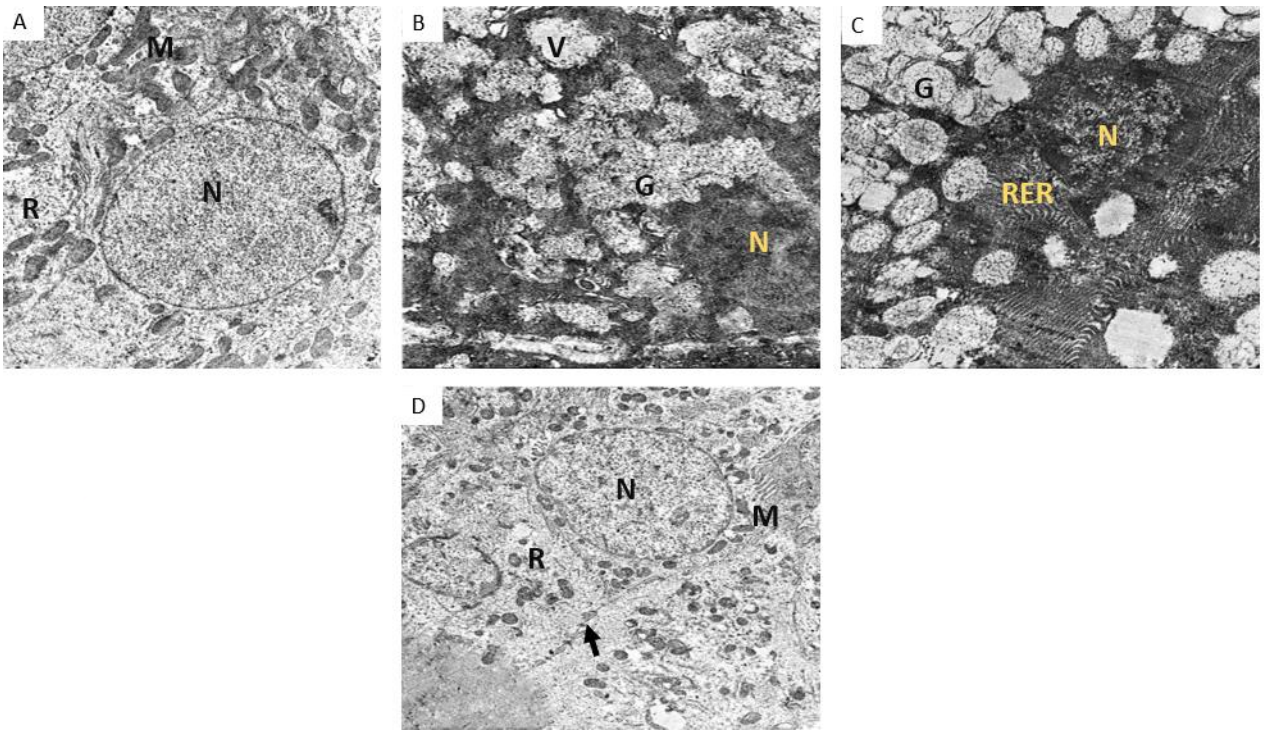

Figure 4 (A): An electron micrograph of the control group showing a serous secretory cell with nucleus (N), Mitochondria (M), and free ribosomes (R) (Uranyl acetate & lead citrate x12000), (B): Electron micrograph of cholesterol group showing acinar cells, pyramidal with irregular shrunken nuclei (N), and multiple electro-lucent secretory granules (G) were noticed. Large and small cytoplasmic vacuoles (V) (Uranyl acetate & lead citrate x5000), (C): An electron micrograph of the atorvastatin-treated group showing serous acinar cells with rounded nuclei (N) and rough endoplasmic reticulum (RER). secretory granules were noticed (G). (arrows) (Uranyl acetate & lead citrate x8000), (D): An electron micrograph of serous acini of cinnamon treated group showing a serous acinar cell with rounded nucleus (N), mitochondria (M) lateral interdegitations were noticed (Uranyl acetate & lead citrate x12000).

5. Conclusions

Hypercholesterolemia severely affects the structure of the salivary glands to different degrees. Administration of Atorvastatin as a synthetic line of treatment for hypercholesterolemia positively affected submandibular gland tissue and the cholesterol level in the blood. As a natural herbal line of treatment Cinnamon enhanced the histological and ultrastructure picture of the submandibular gland, level of caspase III in addition to blood cholesterol levels in hypercholesteraemic rats.

References

[1] L. A. Woollett. (2011). Transport of maternal cholesterol to the fetal circulation. Placenta. 32: S218–S221.

[2] M. Nayor, R. S. Vasan. (2016). Recent Update to the US Cholesterol Treatment Guidelines: A Comparison With International Guidelines. Circulation. 133 (18): 1795–1806.

[3] S. Qiu, W. Zhuo, C. Sun, Z. Su, A. Yan, L. Shen. (2017). Effects of atorvastatin on chronic subdural hematoma: A systematic review. Medicine. 96 (26): e7290.

[4] F. Heydarpour, N. Hemati, A. Hadi, S. Moradi, E. Mohammadi, M. H. Farzaei. (2020). Effects of cinnamon on controlling metabolic parameters of polycystic ovary syndrome: A systematic review and meta-analysis. Journal of ethnopharmacology. 254: 112741.

[5] S. M. Turbino-Ribeiro, M. E. Silva, D. A. Chianca, H. J. De Paula, L. M. Cardoso, E. Colombari, M. L. Pedrosa. (2003). Iron overload in hypercholesterolemic rats affects iron homeostasis and serum lipids but not blood pressure. The Journal of nutrition. 133 (1): 15–20.

[6] O. Uličná, O. Vančová, I. Waczulíková, P. Božek, L. Šikurová, V. Bada, J. Kucharská. (2012). Liver mitochondrial respiratory function and coenzyme Q content in rats on a hypercholesterolemic diet treated with atorvastatin. Physiological research. 61 (2): 185–193.

[7] I. Zahid, A. Taseer, A. Aamir. (2016). Antihyperlipidemic efficacy of cinnamon in albino rats. Asian Journal of Agricultural Biology. 4 (1): 8-16.

[8] D. González-Peña, J. Angulo, S. Vallejo, C. Colina-Coca, B. de Ancos, C. F. Sánchez-Ferrer, C. Peiró, C. Sánchez-Moreno. (2014). High-cholesterol diet enriched with onion affects endothelium-dependent relaxation and NADPH oxidase activity in mesenteric microvessels from Wistar rats. Nutrition & metabolism. 11: 57.

[9] P. Khosla, K. Sundram. (1996). Effects of dietary fatty acid composition on plasma cholesterol. Progress in lipid research. 35 (2): 93–132.

[10] U. Ahmad, R. S. Ahmad, M. S. Arshad, Z. Mushtaq, S. M. Hussain, A. Hameed. (2018). Antihyperlipidemic efficacy of aqueous extract of Stevia rebaudiana Bertoni in albino rats. Lipids in health and disease. 17: 1-8.

[11] R. Pışırıcıler, E. Çalişka-Ak, E. Emeklı-Alturfan, A. Yarat, Y. Canberk. (2009). Impact of Experimental Hyperlipidemia on Histology of Major Salivary Glands. Medical Journal of Trakya University/Trakya Universitesi Tip Fakultesi Dergisi. 26 (4).

[12] T. Henics, D. N. Wheatley. (1999). Cytoplasmic vacuolation, adaptation and cell death: a view on new perspectives and features. Biology of the cell. 91 (7): 485–498.

[13] R. Moubarak. (2008). The effect of hypercholesterolemia on the rat parotid salivary gland (histopathological and immunohistochemical study). Cairo Dental Journal. 24 (1): 19-28.

[14] A. A. Starkov, K. B. Wallace. (2002). Structural determinants of fluorochemical-induced mitochondrial dysfunction. Toxicological sciences: an official journal of the Society of Toxicology. 66 (2): 244–252.

[15] A. H. Wagner, T. Köhler, U. Rückschloss, I. Just, M. Hecker. (2000). Improvement of nitric oxide-dependent vasodilatation by HMG-CoA reductase inhibitors through attenuation of endothelial superoxide anion formation. Arteriosclerosis, thrombosis, and vascular biology. 20 (1): 61–69.

[16] S. A. Selim. (2013). The effect of high-fat diet-induced obesity on the parotid gland of adult male albino rats: histological and immunohistochemical study. Egyptian Journal of Histology. 36 (4): 772-780.

[17] A. Wierzbicki. (2001). Atorvastatin. Expert Opin Pharmacotherapy. 2 (5): 819–830.

[18] J. A. Young, E. W. Van Lennep. (1979). Transport in salivary and salt glands. In Transport organs (pp. 563-692). Berlin, Heidelberg: Springer Berlin Heidelberg.

[19] Z. Alikhani, M. Alikhani, C. M. Boyd, K. Nagao, P. C. Trackman, D. T. Graves. (2005). Advanced glycation end products enhance expression of pro-apoptotic genes and stimulate fibroblast apoptosis through cytoplasmic and mitochondrial pathways. The Journal of biological chemistry. 280 (13): 12087–12095.

[20] F. J. Raal, G. J. Pilcher, D. R. Illingworth, A. S. Pappu, E. A. Stein, P. Laskarzewski, Y. B. Mitchel, M. R. Melino. (1997). Expanded-dose simvastatin is effective in homozygous familial hypercholesterolemia. Atherosclerosis. 135 (2): 249-256.

[21] M. H. Jang, M. C. Shin, H. S. Shin, K. H. Kim, H. J. Park, E. H. Kim, C. J. Kim. (2002). Alcohol induces apoptosis in TM3 mouse Leydig cells via bax-dependent caspase-3 activation. European journal of pharmacology. 449 (1-2): 39–45.

[22] M. M. AL-Rawi. (2007). Efficacy of oat bran (Avena sativa L.) in comparison with atorvastatin in the treatment of hypercholesterolemia in albino rat liver. The Egyptian Journal of Hospital Medicine. 29 (1): 511-521.

[23] E. Sehayek, E. Butbul, R. Avner, H. Levkovitz, S. Eisenberg. (1994). Enhanced cellular metabolism of very low density lipoprotein by simvastatin. A novel mechanism of action of HMG-CoA reductase inhibitors. European journal of clinical investigation. 24 (3): 173–178.

[24] A. Gaw, C. J. Packard, E. F. Murray, G. M. Lindsay, B. A. Griffin, M. J. Caslake, B. D. Vallance, A. R. Lorimer, J. Shepherd. (1993). Effects of simvastatin on apoB metabolism and LDL subfraction distribution. Arteriosclerosis and thrombosis : a journal of vascular biology. 13 (2): 170–189.

[25] G. M. Kostner, D. Gavish, B. Leopold, K. Bolzano, M. S. Weintraub, J. L. Breslow. (1989). HMG CoA reductase inhibitors lower LDL cholesterol without reducing Lp(a) levels. Circulation. 80 (5): 1313–1319.

[26] A. D. Marais, R. P. Naoumova, J. C. Firth, C. Penny, C. K. Neuwirth, G. R. Thompson. (1997). Decreased production of low density lipoprotein by atorvastatin after apheresis in homozygous familial hypercholesterolemia. Journal of lipid research. 38 (10): 2071–2078.

[27] A. H. Wagner, T. Köhler, U. Rückschloss, I. Just, M. Hecker. (2000). Improvement of nitric oxide-dependent vasodilatation by HMG-CoA reductase inhibitors through attenuation of endothelial superoxide anion formation. Arteriosclerosis, thrombosis, and vascular biology. 20 (1): 61–69.

[28] U. Laufs, V. L. Fata, J. Plutzky, J. K. Liao. (1998). Upregulation of endothelial nitric oxide synthase by HMG CoA reductase inhibitors. Circulation. 97 (12): 1129–1135.

[29] E. Pan, S. J. Nielsen, A. Mennander, E. Björklund, A. Martinsson, M. Lindgren, E. C. Hansson, A. Pivodic, A. Jeppsson. (2022). Statins for secondary prevention and major adverse events after coronary artery bypass grafting. The Journal of thoracic and cardiovascular surgery. 164 (6): 1875-1886.

[30] B. A. Diebold, N. V. Bhagavan, R. J. Guillory. (1994). Influences of lovastatin administration on the respiratory burst of leukocytes and the phosphorylation potential of mitochondria in guinea pigs. Biochimica et biophysica acta. 1200 (2): 100–108.

[31] K. Nakahara, M. Kuriyama, Y. Sonoda, H. Yoshidome, H. Nakagawa, J. Fujiyama, I. Higuchi, M. Osame. (1998). Myopathy induced by HMG-CoA reductase inhibitors in rabbits: a pathological, electrophysiological, and biochemical study. Toxicology and applied pharmacology. 152 (1): 99–106.

[32] K. Satoh, K. Ichihara. (2000). Lipophilic HMG-CoA reductase inhibitors increase myocardial stunning in dogs. Journal of cardiovascular pharmacology. 35 (2): 256–262.

[33] H. K. Berthold, S. Unverdorben, R. Degenhardt, M. Bulitta, I. Gouni-Berthold. (2006). Effect of policosanol on lipid levels among patients with hypercholesterolemia or combined hyperlipidemia: a randomized controlled trial. JAMA. 295 (19): 2262–2269.

[34] U. Anilkumar, J. H. Prehn. (2014). Anti-apoptotic BCL-2 family proteins in acute neural injury. Frontiers in cellular neuroscience. 8: 281.

[35] S. Kumar. (2007). Caspase function in programmed cell death. Cell Death and Differentiation. 14 (1): 32-43.

[36] T. L. Chen, G. L. Zhu, X. L. He, J. A. Wang, Y. Wang, G. A. Qi. (2014). Short-term pretreatment with atorvastatin attenuates left ventricular dysfunction, reduces infarct size and apoptosis in acute myocardial infarction rats. International journal of clinical and experimental medicine. 7 (12): 4799–4808.

[37] U. Anilkumar, J. H. Prehn. (2014). Anti-apoptotic BCL-2 family proteins in acute neural injury. Frontiers in cellular neuroscience. 8: 281.

[38] A. Khan, M. Safdar, M. M. A. Khan, K. N. Khattak, R. A. Anderson. (2003). Cinnamon improves glucose and lipids of people with type 2 diabetes. Diabetes care. 26 (12): 3215–3218.

[39] S. N. Abd El-Rahman, A. M. Abdel-Haleem, H. M. A. Mudhaffar. (2010). Anti-diabetic effect of cinnamon powder and aqueous extract on rats. International Journal of Food, Nutrition and Public Health. 3 (2): 183-186.

[40] S. M. Kassaee, M. T. Goodarzi, E. A. Oshaghi. (2017). Renoprotective Effects of Trigonella foenum and Cinnamon on Type 2 Diabetic Rats. Avicenna Journal of Medical Biochemistry. 5 (1): 17-21.